

Facsimile Price \$ 3.60
Microfilm Price \$ 1.40
Available from the
Office of Technical Services
Department of Commerce
Washington 25, D. C.

GEAP-4313
Informal AEC Research
and Development Report
February, 1964

SODIUM MASS TRANSFER: VIII
CORROSION OF STAINLESS STEEL IN
ISOTHERMAL REGIONS OF A FLOWING SODIUM SYSTEM

by

J. D. Mottley

Prepared for the
SODIUM COMPONENTS DEVELOPMENT PROGRAM
of the
UNITED STATES ATOMIC ENERGY COMMISSION
UNDER CONTRACT AT(04-3)-189
PROJECT AGREEMENT NO. 15

Printed in U. S. A. Price \$1.00. Available from the
Office of Technical Services, Department of Commerce
Washington 25, D. C.

VALLECITOS ATOMIC LABORATORY

GENERAL  ELECTRIC
ATOMIC POWER EQUIPMENT DEPARTMENT
SAN JOSE, CALIFORNIA

TABLE OF CONTENTS

		<u>Page</u>
	PREFACE	iv
I	INTRODUCTION	1
II	SYSTEM DESCRIPTION	2
III	CORROSION MECHANISM POSTULATION	7
IV	A REVIEW OF ASSUMPTIONS MADE IN MECHANISTIC AND ANALYTICAL TREATMENT	16
	A. Mechanism	16
	B. Analytical	16
V	RESULTS	16
VI	DISCUSSION OF RESULTS	20
VII	CONCLUSIONS	23
VIII	ACKNOWLEDGMENTS	23
<u>APPENDIX</u>		
A	TABLES OF LOOP OPERATING CONDITIONS AND CORROSION DATA	24
B	CALCULATIONS OF DIFFUSION COEFFICIENT AND CONCENTRATIONS OF IRON OXIDE IN SODIUM	28
	NOMENCLATURE	31
	REFERENCES	32

LIST OF ILLUSTRATIONS

<u>Figure</u>	<u>Title</u>	<u>Page</u>
1	Loop Arrangement	3
2	Typical Hot Leg Sample Holder	4
3	Schematic Sketch of Corrosion Sample Position In Isothermal Region	6
4	Volume Element Over Which Mass Balance Is Made To Obtain Differential Equations for the Concentration Profile in Sodium In the Region of the Wall or Specimen	10
5	Corrosion Data Correlation - Run 1-3	17
6	Corrosion Data Correlation - Run 3-7	18
7	Corrosion Data Correlation - Run 4-4	19

LIST OF TABLES

<u>Table</u>	<u>Title</u>	<u>Page</u>
I	Data Origin	2
II	Solubility of Fe (as FeO) g/g Na	8
III	Calculated ΔC , g Fe (as FeO)/g Na	20
IV	Loop Operating Parameters and Materials of Construction	24
V	Run 1-3 Sample Location and Corrosion Rates	25
VI	Run 3-7 Sample Location and Corrosion Rates	26
VII	Run 4-4 Sample Location and Corrosion Rates	27
VIII	Calculated Concentration Difference Values $\Delta C = C_o - C_{E1}$	29

PREFACE

By Leo F. Epstein

November 1, 1963

This report, by J. D. Mottley, is primarily concerned with exploring the physical nature and the mechanism of the so-called isothermal "downstream" effect. In the course of this development, however, the author has introduced some bold and provocative concepts with implications that go far beyond the immediate problem under consideration.

Whether this explanation of the change in corrosion behavior in an isothermal region with respect to the fluid flow is an accurate description of the process remains to be explored further. Certainly the quantitative agreement that will be noted in Figures 5 to 7 is such as to suggest that a considerable degree of confidence may be placed in the approach and the results presented here. However, the sample-holder configurations are sufficiently complex and there is enough basis for arbitrary choice in this treatment (for example, in the selection of the origin for the coordinate system) that many more examples will have to be subjected to a detailed analysis by these methods before the complete validity of the approach is established.

The assumptions and postulates which enter into this analysis are rather startling in themselves. Mottley assumes that the species responsible for the corrosion behavior in an iron base system is FeO or a complex of this compound with Na₂O. Simpler (and certainly more naive) analyses of liquid metal corrosion phenomena have treated them as ordinary solution processes. Two alternate hypotheses have been developed to explain the kinetics of solution or corrosion. In the first, the rate-determining process is the diffusion of the metal dissolved in the liquid phase (as in the case of Fe in Hg). The second hypothesis explains the corrosion process as the result of a series of chemical reactions and physical steps, and the rate in this case may be determined by chemical kinetic as well as physical transport relations. This latter case has been referred to as "solution-rate" limited, in contrast to the first concept which has been called "diffusion-rate" limited [4]. For iron in sodium, only the solution-rate process, the second of these explanations seems credible. Using the fact that diffusion rates of solutes in liquid metals do not depart widely from a value of about 10^{-4} cm²/sec and the measurements of the equilibrium solubility of Fe in Na [3, 5, 9], a diffusion model predicts incredibly high values for the corrosion rate to be expected by this mechanism. By using the much lower solubilities obtained at NRL [1], the diffusion model yields corrosion rates which are more nearly consistent with observation. This fact has led some observers to prefer the lower solubility values, in spite of the contradictory results of three other laboratories. Even this simplification has not been sufficient to explain the experimental observations. If the process takes place by a diffusion mechanism, the very large effect of oxygen on the corrosion rate seems inexplicable: it is not easy to imagine

that oxygen in solution at the parts per million level could have the drastic effect on the diffusion coefficient of metallic Fe dissolved in Na or on the physical properties of the fluid (viscosity, density, etc.), which the corrosion data would appear to demand. Thus the diffusion postulate, even with the low NRL solubility data, cannot adequately explain the over-all observations on corrosion.

In recent years, new information has been developed which makes some aspects of the solution-rate hypothesis a little puzzling. For example, extensive studies in this program have indicated that the dependence of the hot zone corrosion rate on the linear flow velocity, v , is given by an expression* in $v^{0.76 \pm 0.18}$, in excellent agreement with the $v^{0.8}$ relation predicted by diffusion theory. This then would suggest the diffusion concept is the valid one, and not the solution rate formulation. But, as was outlined above, there are very real and substantial objections to the simple diffusion theory.

Faced with the breakdown of both of these concepts, by the arguments given above, Mottley assumes that the true process is neither of the elementary ones previously postulated. The rate determining step is, he says, truly diffusion (thus accounting for the $v^{0.8}$ behavior), not of dissolved iron, but rather of FeO or some related species in solution. Since the bulk iron phase can be converted into the required FeO only by a chemical reaction, this process is also, in a sense, solution-rate controlled. By assuming that the iron in solution exists in the forms (1) free atoms or ions of Fe and (2) as FeO, either in simple or complex form, in a single bold stroke Mottley has caused virtually all of the puzzling incompatibilities present in the earlier arguments to vanish.

He then goes on to make the assumption that the Fe solubility measurements of KAPL, MSA and ANL yielded the total iron content present in the solutions; while the NRL data represented only the iron present in the oxide complex. Why this should be, he does not venture to suggest; it is implied that some obscure aspects of the radiochemical technique used at the Navy laboratory were responsible for this result. Here, once more, is a rather Alexandrian cutting of the Gordian Knot. By this one postulate, the long-standing discrepancy on the iron solubility results is resolved - a conflict that has existed to puzzle, annoy and irritate workers in this field for over ten years.

He proceeds to incorporate these assumptions, the direct evidence for which is virtually non-existent, into a mathematical theory with some degree of sophistication. And most amazingly, the theory (1) checks experimental observations (see Figures 5 to 7) and (2) leads to predictions on the magnitude of the concentration difference, ΔC , that are in good agreement (see Table III,

*See section VI D of GEAP-3726 Vol. 1. "Sodium Mass Transfer: II Screening Test Data and Analysis" - Mass Transfer Results compiled by R. W. Lockhart, where it is stated that, for hot leg observations "The exponent for velocity did not vary significantly among loops or between runs.....The average velocity exponent is 0.76 ± 0.18 ".

p. 20) with the NRL results interpreted in this very special way. These facts, then, demand a certain amount of respect for and serious consideration of the otherwise apparently rather imaginative and far-fetched assumptions entering into the theory.

The development is, as is most often the case, over-simplified in detail, and this is undoubtedly responsible for the deviations from observation which occur. For example, this paper predicts that R , the dynamic corrosion rate, should vary as $v^{1/2}$, the square root of the flow velocity, rather than the 0.8 power (see eq. (11) and (22)). The higher exponent which is closer to that found experimentally, is the result of dimensional analysis and the application of the mass transfer-heat transfer analogy for fully turbulent flow which leads to the familiar heat transfer result^[4]

$$Nu = 0.023 Re^{0.8} Pr^{0.4}$$

This difference between a $v^{0.5}$ and a $v^{0.8}$ relation probably arises from the over-simplified expression chosen in this paper for the velocity distribution across the flow path

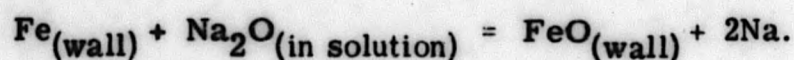
$$v_x(y) = \begin{cases} 0 & \text{for } y < \delta \\ \bar{v} & \text{for } y \geq \delta \end{cases}$$

It is known from other studies that the sharp discontinuity at $y = \delta$ implied by this relation is not physically accurate, and that, for round tubes of radius, R , at least, the expression^[2, p. 155]

$$v_x(y) = \bar{v} (y/R)^{1/7}, \quad 0 \leq y \leq R$$

conforms more closely to experimental observation. The use of this expression in the partial differential equation (8) however, leads to forms that can be evaluated analytically only with extreme difficulty, if at all, and the solution with this velocity profile can probably be obtained only by approximation methods. Use of such techniques in this case would probably be less desirable, in that the functional relations between the variables, and the dependence of the corrosion rate on quantities such as flow velocity, position, etc. would not be so clearly delineated as they are in the method of treatment used above.

There is one other conclusion that can be derived from this treatment which is extremely interesting and important in its implications. It has for a long time been assumed that the corrosion rate of iron in sodium containing oxygen is a linear function of the oxygen content^[4, p. 76] although the amount and quality of the evidence supporting this concept has been distressingly meager. (Recent work has suggested that the corrosion of other metals by Li, Rb and Cs may also be nearly linear in the oxygen content of the liquid metal.) Note that from equation (11), it is predicted that R is directly proportional to $(C_0 - C_{E1})$, the concentrations at the wall and in the bulk phase, respectively. But this treatment implies that the first step in the corrosion process for clean iron is the reaction



Since both solid iron and sodium are present in huge excess, at unit activity, these do not appear in the equilibrium constant for the reaction

$$K = \frac{C_{\text{FeO}}}{C_{\text{Na}_2\text{O}}}$$

and the concentration of FeO is directly proportional to the Na₂O or oxygen concentration in the system. Thus this treatment most satisfactorily predicts the linear dependence of corrosion rate on oxygen content.

The analysis of the "downstream effect" in this paper, therefore, has opened up some entirely new vistas in the theory of liquid metal corrosion, some of which may be of much greater importance than the geometric factor directly considered. The treatment is vulnerable, as has been noted above. In particular, some experimental confirmation supporting the idea that the NRL solubility measurements in fact measured only dissolved iron in the oxide compound form would be most desirable since this is a hypothesis which is contrary to views of many qualified workers in the field. But the agreement with experiment noted here and the compatibility of the constants obtained with observation (see Table III) must command, if not agreement, at least respectful attention and careful consideration in the further development of the theory of liquid metal corrosion.

CORROSION OF STAINLESS STEEL IN
ISOTHERMAL REGIONS OF A FLOWING SODIUM SYSTEM

I. INTRODUCTION

The successful use of liquid sodium as a nuclear reactor coolant is dependent upon the lifetimes of the piping and components of the system with which the sodium comes in contact. In the coolant system, sodium leaves the reactor at a high temperature and enters a heat exchanger where heat is removed. Because of the temperature differential in the system, mass transport of material from piping and system components can occur between hot and cold regions.

Corrosion - the removal of material (primarily in the hot region), and deposition - the addition of material to the system walls (mainly in the cold region), are functions of many system parameters.

- a. System materials of construction.
- b. System geometry and dimensions.
- c. Temperature distribution throughout the loop.
- d. Impurities (e.g., sodium oxide) which affect corrosion rates.
- e. Operating age of the system.
- f. Sodium flow rate.

At the General Electric Company's Atomic Power Equipment Department (APED), six heat transfer loops have been constructed under U. S. Atomic Energy Commission Contract AT(04-3)-189 Project Agreement 15 for studying the corrosion and transfer of alloying constituents from different materials of construction (316 stainless steel, 2 $\frac{1}{4}$ Cr - 1 Mo and 5 Cr - $\frac{1}{2}$ Mo - $\frac{1}{2}$ Ti steel alloy). The primary purpose of this paper is to formulate a rationally derived analytical expression which can predict the effect of sodium flow velocity and of position - with respect to the flow path ("downstream effect") - on local corrosion rates in isothermal regions.

To solve this problem a mechanism of corrosion is assumed and a mathematical model describing the physical processes is formulated. The isothermal regions where corrosion data are taken in the sodium mass transfer (SMT) loops are of complicated geometry (many bends, expansions, and contractions), and a description of a typical isothermal region will be given first with the assumptions concerning system geometry necessary to set up a mathematical model.

II. SYSTEM DESCRIPTION

In Figure 1, a schematic drawing of the loop arrangement [7] is shown. The part of the system which is of interest in this study includes the hot region from heater #1 to the H3R sample holder. During operation the sample holder H1 is operated at 1000 F, H2 at 1100 F, and H3 and H3R at 1200 F. In one special run (loop 4, Run 4) where a long isothermal region at 1200 F was desired all hot leg holders were operated at 1200 F.

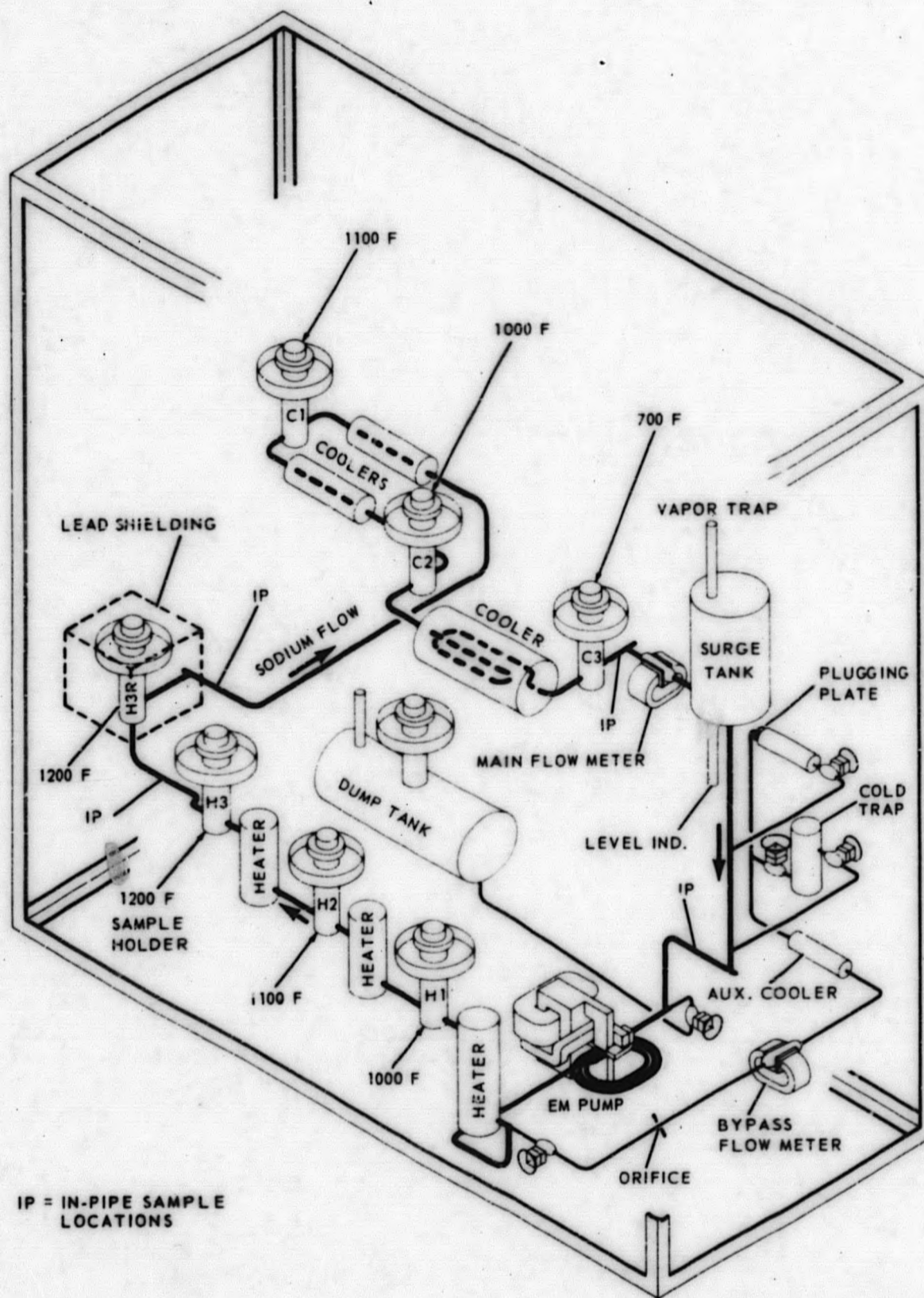
A partially exploded view of a typical sample holder [7] is illustrated in Figure 2. All components of the sample holder exposed to sodium are machined from bar stock of the same material as that selected for that particular section of the loop. Two different slot (coolant passage) configurations are utilized for the sample holder insert design. The dimensions are based on 1 gpm loop flow with a corrosion sample located within the slot. With the standard corrosion sample inserted, slots 0.115 inch wide by 0.180 inch deep give a sodium velocity of 30 fps with one passage per insert and 10 fps with three parallel passages per insert.

In loop operation, sample holders H3 and H3R are operated at 1200 F, and four sets of data are available as shown in Table I.

TABLE I

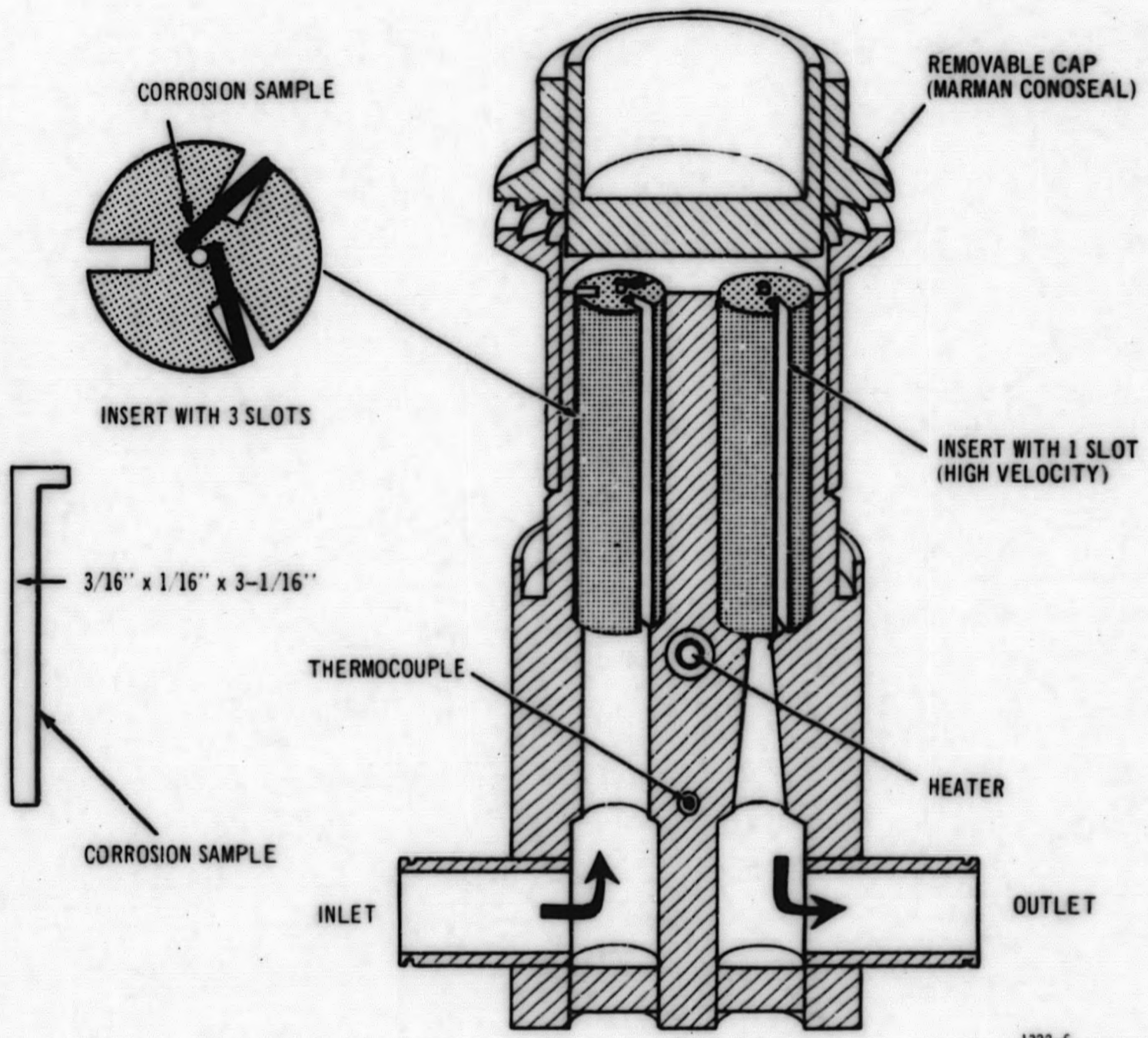
<u>Position</u>	<u>Number of Samples</u>	<u>Velocity</u>	<u>Downstream Position</u>
H3 Inlet	3	Low	1
H3 Outlet	1	High	2
H3R Inlet	3	Low	3
H3R Outlet	1	High	4

Corrosion data at 1200 F are analyzed in this paper because of the larger number of downstream positions at this temperature than at either 1100 F or 1000 F. A position $x = 0$ is chosen for the isothermal region of 1200 F to provide an origin from which the downstream distance can be measured. This position was selected at the location in the loop where the 1100 F region ended. In Runs 1-3 and 3-7 this is the inlet to heater #3. In Run 4-4 a linear temperature gradient was assumed in heater #1 and the point where $T = 1100$ F was chosen as $x = 0$. Strictly, with this selection as an origin, the whole region to be analyzed is not isothermal. Because of the high thermal conductivity of sodium, however, a 1200 F temperature will be obtained not far from the origin.



1322-7

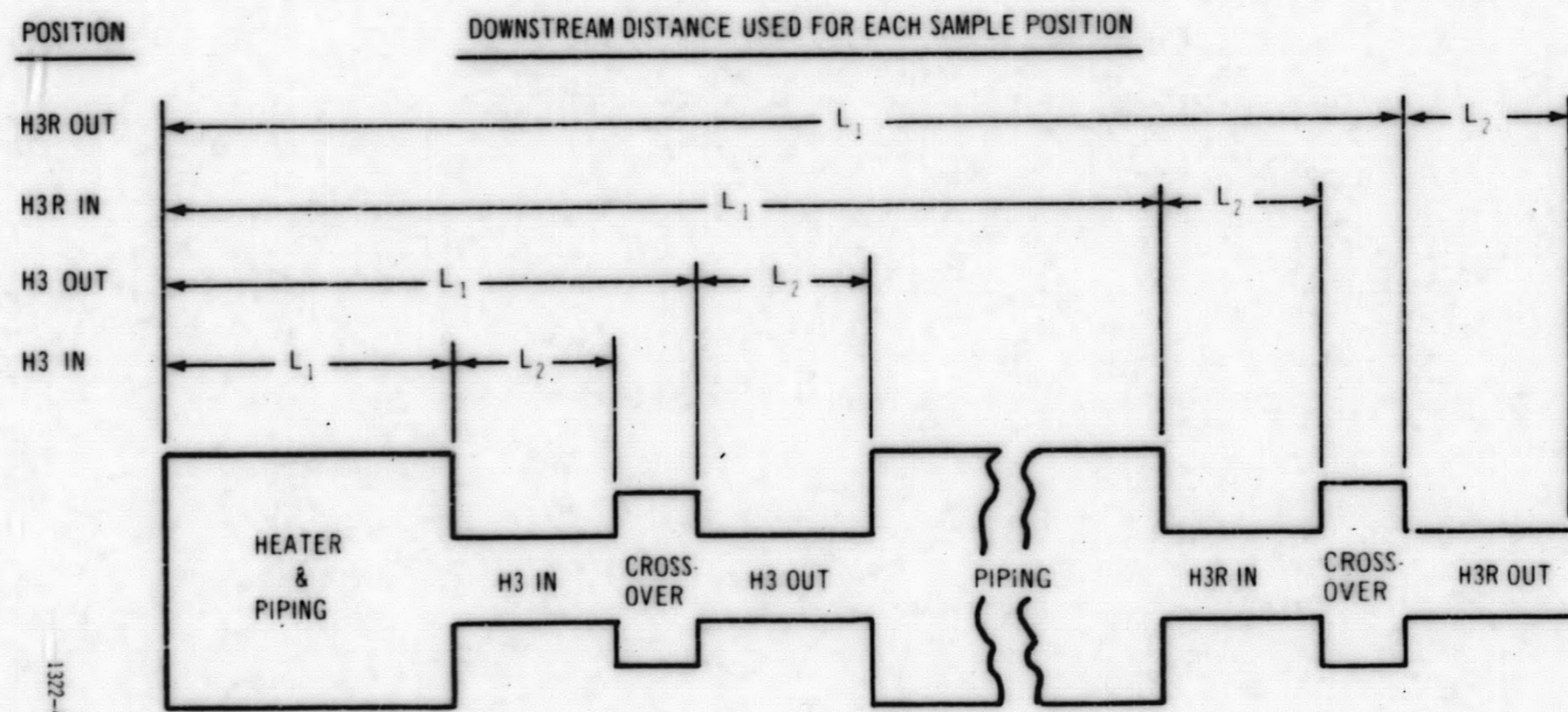
Figure 1. Loop Arrangement



1322-6

Figure 2. Typical Hot Leg Sample Holder

As can be seen from Figure 2, the sample holder geometry and piping configuration preceding the sample holder are complicated. Formulation of a mathematical model describing corrosion requires a simplified picture. Therefore, the isothermal region was broken down into two sections for any corrosion sample which was to be analyzed: Section I which included all piping and sample holders from $x = 0$ to the point preceding the sample, and Section II the corrosion sample. A sketch of Section I and Section II for the four downstream positions is shown in Figure 3.



1322-4

Figure 3. Schematic Sketch of Corrosion Sample Position In Isothermal Region

GEAP-4313

III. CORROSION MECHANISM POSTULATION

Mathematical formulation of a corrosion rate requires a mechanism by which mass can be transferred from the wall or sample specimen into the flowing sodium stream. Chromium, nickel, and other constituents are present in stainless steel, and some of these products are known to be selectively extracted by sodium. However, the gross mass transfer effects observed can be treated by assuming that wall (solid) transport phenomena are not rate limiting at the steady state. Therefore, the problem may be evaluated as though iron were the only material involved.

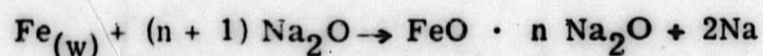
Evidence has been obtained which shows that the corrosion rate of iron is proportional to the sodium oxide concentration in the sodium. [4] Any mechanism of corrosion must take this into account.

The following mechanistic steps are assumed to take place in the corrosion process:

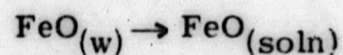
- a. Sodium oxide, Na_2O diffuses from the bulk sodium stream to the wall.
- b. It reacts rapidly with the iron of the wall to form iron oxide or an iron oxide-sodium oxide complex. [6]



or



- c. The iron oxide or complex goes into solution



- d. The FeO or complex in solution diffuses into the bulk stream (rate determining step).

For purposes of discussion, iron oxide, FeO, is taken as the corroding species, although an iron oxide complex could be substituted with no loss of meaning. The rate limiting step is assumed to be the diffusion of iron oxide into the bulk sodium stream. The following assumptions are also made:

- a. The FeO concentration in sodium at the wall is the equilibrium FeO concentration and is dependent upon the sodium oxide concentration.
- b. FeO diffuses across a film of thickness δ ; the concentration at δ at the entrance of any section being the concentration of the entering bulk FeO in that section.
- c. Steady-state conditions are assumed.

An estimate of the equilibrium iron oxide concentration in sodium can be obtained from data of solubilities of iron in sodium.^[1] In reference [1] two sets of data are given: the first, that of iron solubility as a function of temperature with essentially no sodium oxide present.

$$\text{grams Fe/gram Na} = 2.28 \times 10^{-9} - 1.63 \times 10^{-11} T + 5.63 \times 10^{-14} T^2 \quad (\text{A})$$

where T is expressed in degrees Centigrade. A second set of data gives "the solubility of iron in sodium metal saturated with Na₂O" as a function of temperature and can be represented by the expression

$$\text{grams Fe gram Na} = 3.17 \times 10^{-8} - 1.71 \times 10^{-10} T + 3.51 \times 10^{-13} T^2 \quad (\text{B})$$

where T is in degrees Centigrade. Since the solubility of iron as metallic iron in sodium would not be expected to be dependent on sodium oxide concentration, the excess iron in solution when sodium oxide is present must be in some iron-oxygen compound. An expression for the concentration of iron as an iron-oxygen compound (FeO) in sodium can be formulated by subtracting equation (A) from equation (B).

$$\text{grams Fe as FeO/gram Na} = 2.94 \times 10^{-8} - 1.55 \times 10^{-10} T + 2.95 \times 10^{-13} T^2 \quad (\text{C})$$

where T is in degrees Centigrade.

In Table II, values of Fe as FeO are given as a function of temperature, derived from equation (C)

TABLE II

Solubility of Fe as FeO g/g Na

Temperature °C	Temperature °F	g Fe as FeO/gram Na
200	392	1.02×10^{-8}
300	572	0.54×10^{-8}
400	752	1.46×10^{-8}
450	842	1.96×10^{-8}
500	932	2.56×10^{-8}
550	1022	3.34×10^{-8}
600	1112	4.26×10^{-8}
650	1202	5.33×10^{-8}
700	1292	6.57×10^{-8}

Values above about 550 C are extrapolated.

The differential equations are now set up to describe the corrosion process with the diffusion of iron oxide as the rate limiting step. First, a mass balance for iron oxide is established. The concentration of iron oxide C , will change with y , the distance into the stream from the wall or the corrosion sample, and x , the distance downstream from some initial starting point $x = 0$. For the element of volume (see Figure 4) over which the mass balance is set up, the volume formed by the intersection of a slab of thickness Δx with a slab of thickness Δy is selected. [2] The mass balance on iron oxide in the steady state is simply

$$N_x|_x w \Delta y - N_x|_{x + \Delta x} w \Delta y + N_y|_y w \Delta x - N_y|_{y + \Delta y} w \Delta x = 0 \quad (1)$$

where

w = the width of the sample or wall

$N_x|_x$ and $N_x|_{x + \Delta x}$ = mass flux of iron oxide in x direction at position x and $x + \Delta x$

$N_y|_y$ and $N_y|_{y + \Delta y}$ = mass flux of iron oxide in y direction at position y and $y + \Delta y$

By dividing by $w \Delta x \Delta y$ and passing to the limit as the volume element becomes infinitesimally small, the equation

$$\frac{\partial N_x}{\partial x} + \frac{\partial N_y}{\partial y} = 0 \quad (2)$$

is obtained.

For the mass flux in the x direction

$$N_x = -D \frac{\partial C}{\partial x} + z N_{Na_x} \quad (3)$$

where

D = the diffusion coefficient of iron oxide in liquid sodium

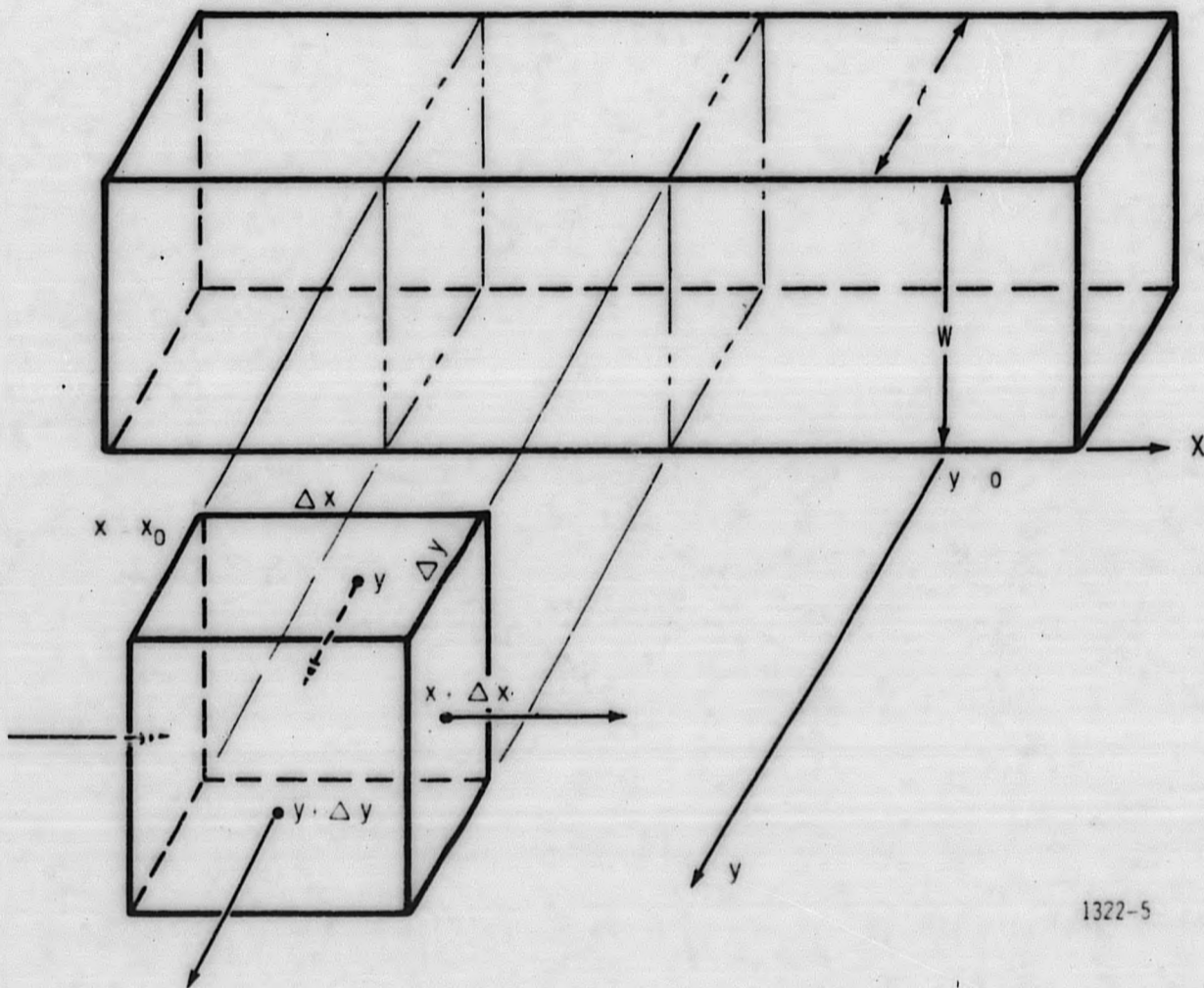
z = the mass fraction of iron oxide

N_{Na_x} = mass flux of the liquid sodium.

Since diffusion is negligible in the direction of flow

$$N_x = C v_x(y) \quad (4)$$

$v_x(y)$ = linear flow velocity in x direction, ft/sec., a function of y .



1322-5

Figure 4. Volume Element Over Which Mass Balance Is Made To Obtain Differential Equations For The Concentration Profile In Sodium In The Region Of The Wall or Sample Specimen

The mass flux in the y direction is given by

$$N_y = -D \frac{\partial C}{\partial y} + z N_{Na_y} \quad (5)$$

Since the solubility of iron oxide in liquid sodium is very small, mass transport by convective processes is negligible and

$$N_y = -D \frac{\partial C}{\partial y} \quad (6)$$

Substitution of equations (4) and (6) into equation (2) gives

$$v_x(y) \frac{\partial C}{\partial x} = D \frac{\partial^2 C}{\partial y^2} \quad (7)$$

Equation (7) is the differential equation describing C as a function of x and y. To solve this equation, the expression for $v_x(y)$ must be known. The flow through the sample slots is turbulent as it is in any part of the loop. In this treatment of the problem a flat velocity profile is assumed in every part of the loop and $v_x(y) = v_x$ (average) = v.

Equation (7) becomes:

$$v \frac{\partial C}{\partial x} = D \frac{\partial^2 C}{\partial y^2} \quad (8)$$

with the boundary conditions

$$\begin{aligned} \text{B. C. 1} & \quad C = C_{E1} \text{ at } x = 0 \\ \text{B. C. 2} & \quad C = C_o \text{ at } y = 0 \\ \text{B. C. 3} & \quad C = C_{E1} \text{ at } y = x \end{aligned}$$

where

$$\begin{aligned} C_{E1} & = \text{the entering iron oxide concentration at } x = 0, \text{ g/cm}^3 \\ C_o & = \text{the iron oxide concentration at the wall, g/cm}^3 \end{aligned}$$

In this model it is assumed that a thin film of thickness δ exists next to the wall. At the entrance, $x_i = 0$, of any section i , the iron oxide concentration at $y = \delta$ is assumed to be C_{Ei} , the entering bulk iron oxide concentration. The concentration of iron oxide at the wall at any x is assumed to be proportional to the sodium oxide concentration at that x . In this model it is also assumed that when y is less than δ mass transfer is by diffusion alone. At positions greater than δ , turbulence is present and instantaneous mixing occurs.

Equation (8) is the differential equation for a system of simple geometry, that is a flat plate. In the sample holders the corrosion specimens are essentially flat plates. For computational purposes, the remainder of the piping system is also assumed to be a flat plate. This is approximately correct if the distance which the iron diffuses into the sodium stream is small.

The analytical expression relating the corrosion rate to system geometry and operating variables is obtained from the solution to equation (8). The average concentration of iron oxide at the position $x = L_1$ or the entering point to the corrosion specimen, is first calculated. With this entering concentration as the boundary condition for section II, equation (8) is again solved and the average corrosion rate of the specimen determined.

For the specified boundary conditions the solution to equation (8) for section I is:

$$C_1 = C_o - (C_o - C_{E1}) \operatorname{erf} \frac{y}{(4Dx_1/v_1)^{1/2}} \quad (9)$$

The corrosion rate in section I is:

$$R(x)_1 = +D \left(\frac{\partial C_1}{\partial y} \right)_{y=0} \quad (10)$$

The corrosion rate, R , in $\frac{\text{gram}}{\text{cm}^2\text{-sec}}$ is defined as being negative if the wall or sample specimen loses weight.

Inserting equation (9) into (10)

$$R(x)_1 = +D \left[-(C_o - C_{E1}) \frac{2}{\pi^{1/2}} e^{-\frac{y^2}{(4Dx_1/v_1)}} \frac{1}{(4Dx_1/v_1)^{1/2}} \right]$$

at $y = 0$, $R(x)_1 = -(C_o - C_{E1}) (Dv_1/\pi x_1)^{1/2} \quad (11)$

The average corrosion rate over section I is

$$\begin{aligned}\bar{R}_1 &= \frac{\int_0^{L_1} R(x)_1 dx_1}{L_1} = \frac{-(C_o - C_{E1}) (Dv_1/\pi)^{\frac{1}{2}}}{L_1} \int_0^{L_1} x_1^{-\frac{1}{2}} dx_1 \\ &= -2(C_o - C_{E1})(Dv_1/L_1\pi)^{\frac{1}{2}}\end{aligned}$$

or the average corrosion rate over a distance L_1 is twice the local corrosion rate at $x = L_1$.

It is assumed that at the exit of section I the sodium stream is thoroughly mixed and a new average entering concentration, C_{E2} is present at the entrance to section II. The amount of iron oxide added to solution is calculated by multiplying the average corrosion rate by the exposed surface area and dividing by the volumetric flow rate. This plus the original concentration equals the concentration at the entrance to section II. It is assumed that the exposed surface, S , can be represented by $\pi d_1 L_1$ where d_1 is an effective cross section diameter, of a cylindrical pipe.

$$C_{E2} = C_{E1} - \frac{\pi d_1 L_1 \bar{R}_1}{A_1 v_1} = C_{E1} + \pi \frac{d_1 L_1 \cdot 2(C_o - C_{E1})}{A_1 v_1} \cdot (Dv_1/L_1\pi)^{\frac{1}{2}}$$

Since $A_1 = \frac{\pi d_1^2}{4}$

$$C_{E2} = C_{E1} + \frac{8(C_o - C_{E1})}{d_1} \left(\frac{DL_1}{\pi v_1} \right)^{\frac{1}{2}} \quad (13)$$

The exit concentration from section I is used as the entrance concentration to section II and equation (8) becomes

$$v_2 \frac{\partial C_2}{\partial x} = D \frac{\partial^2 C_2}{\partial y^2} \quad (14)$$

with boundary conditions:

$$\text{B. C. 1 } C_2 = C_{E1} + \frac{8(C_o - C_{E1})}{d_1} \left(\frac{DL_1}{\pi v_1} \right)^{\frac{1}{2}} \text{ at } x = 0$$

$$\text{B. C. 2 } C_2 = C_o \text{ at } y = 0$$

$$\text{B. C. 3 } C_2 = C_{E1} + \frac{8(C_o - C_{E1})}{d_1} \left(\frac{DL_1}{\pi v_1} \right)^{\frac{1}{2}} \text{ at } y = \infty$$

The solution to equation (14) is:

$$C_2 = C_0 - \left\{ C_0 - C_{E1} - \left[\frac{8}{d_1} (C_0 - C_{E1}) \right] \left(\frac{D}{\pi} \right)^{\frac{1}{2}} \left(\frac{L_1}{v_1} \right)^{\frac{1}{2}} \right\} \operatorname{erf} \frac{y}{\left(\frac{4Dx_2}{v_2} \right)^{\frac{1}{2}}} \quad (15)$$

The local corrosion rate of the specimen is:

$$R(x)_2 = +D \left(\frac{\partial C_2}{\partial y} \right)_{y=0} = -(C_0 - C_{E1}) \left(\frac{Dv_2}{\pi x_2} \right)^{\frac{1}{2}} + \frac{8}{d_1} (C_0 - C_{E1}) \frac{D}{\pi} \left(\frac{v_2}{x_2} \frac{L_1}{v_1} \right)^{\frac{1}{2}} \quad (16)$$

The average corrosion rate for the specimen is twice the local corrosion rate at $x = L_2$

$$\therefore \bar{R}_2 = -2(C_0 - C_{E1}) \left(\frac{Dv_2}{\pi L_2} \right)^{\frac{1}{2}} + \frac{16}{d_1} (C_0 - C_{E1}) \frac{D}{\pi} \left(\frac{v_2}{L_2} \cdot \frac{L_1}{v_1} \right)^{\frac{1}{2}} \quad (17)$$

The velocity by the corrosion specimen, $v_2 = kbv_1$ (18)

where $b = \frac{A_1}{A_2}$

A_1 = cross-sectional area of section I

A_2 = cross-sectional area of section II

The constant k , depends upon the number of slots in each sample holder available for flow. For H3R-in, $k = 3$; for H3R-out, $k = 1$.

$$\therefore v_2 = k \frac{A_1}{A_2} v_1 = k \frac{\pi d_1^2}{4 A_2} v_1 \quad (19)$$

Inserting equation (19) into (17)

$$\bar{R}_2 = -2(C_0 - C_{E1}) \left(\frac{Dv_2}{\pi L_2} \right)^{\frac{1}{2}} + 8(C_0 - C_{E1}) \frac{D}{\pi^{\frac{1}{2}}} \left(\frac{k}{A_2} \frac{L_1}{L_2} \right)^{\frac{1}{2}} \quad (20)$$

Since A_2 and L_2 are constant in each sample holder, the measured variables, corrosion rate, velocity, and position can be grouped into two terms

$$\frac{\bar{R}_2}{(kL_1)^{\frac{1}{2}}} = -2(C_0 - C_{E1}) \left(\frac{D}{\pi L_2} \right)^{\frac{1}{2}} \left(\frac{v_2}{kL_1} \right)^{\frac{1}{2}} + 8(C_0 - C_{E1}) \frac{D}{(\pi A_2 L_2)^{\frac{1}{2}}} \quad (21)$$

Equation (21) predicts that a plot of

$$\frac{\bar{R}_2}{(kL_1)^{\frac{1}{2}}} \text{ versus } \left(\frac{v_2}{kL_1} \right)^{\frac{1}{2}}$$

should be a straight line, A_2 and L_2 being constants of the system.

IV. A REVIEW OF ASSUMPTIONS MADE IN MECHANISTIC AND ANALYTICAL TREATMENT

Assumptions:

A. Mechanism

1. Sodium oxide diffusion to wall.
2. Rapid reaction of sodium oxide with iron of wall to form iron oxide or a sodium oxide complex.
3. Iron oxide dissolution in sodium.
4. Diffusion of iron oxide into bulk stream (rate limiting step).

B. Analytical

1. Isothermal region including corrosion sample can be broken down into two sections: section I contains the isothermal region upstream from the corrosion sample, and section II contains the corrosion sample.
2. The residence time for the sodium in sections I and II is short.
3. The area, length, and diameter of section I can be represented by equivalent area, diameter and length of a hollow right circular cylinder.
4. The velocity profile anywhere in the isothermal region may be represented by the average velocity and is not a function of radial position.
5. Steady-state conditions are assumed.
6. Sodium oxide concentration throughout the system is constant under steady-state conditions.

V. RESULTS

Corrosion data on stainless steel samples^[8] exposed at 1200 F and 1100 F from three runs made in three different sodium loops (Runs 1-3, 3-7, and 4-4) were modified according to the form of equation (21) and are plotted in Figures 5-7. (Run 1-3 in Figure 5; Run 3-7 in Figure 6; Run 4-4 in Figure 7.) The loop operating parameters and materials of construction are given in Table IV, Appendix A. The corrosion data sample locations and values of k for each sample position are given in Tables V through VII in Appendix A.

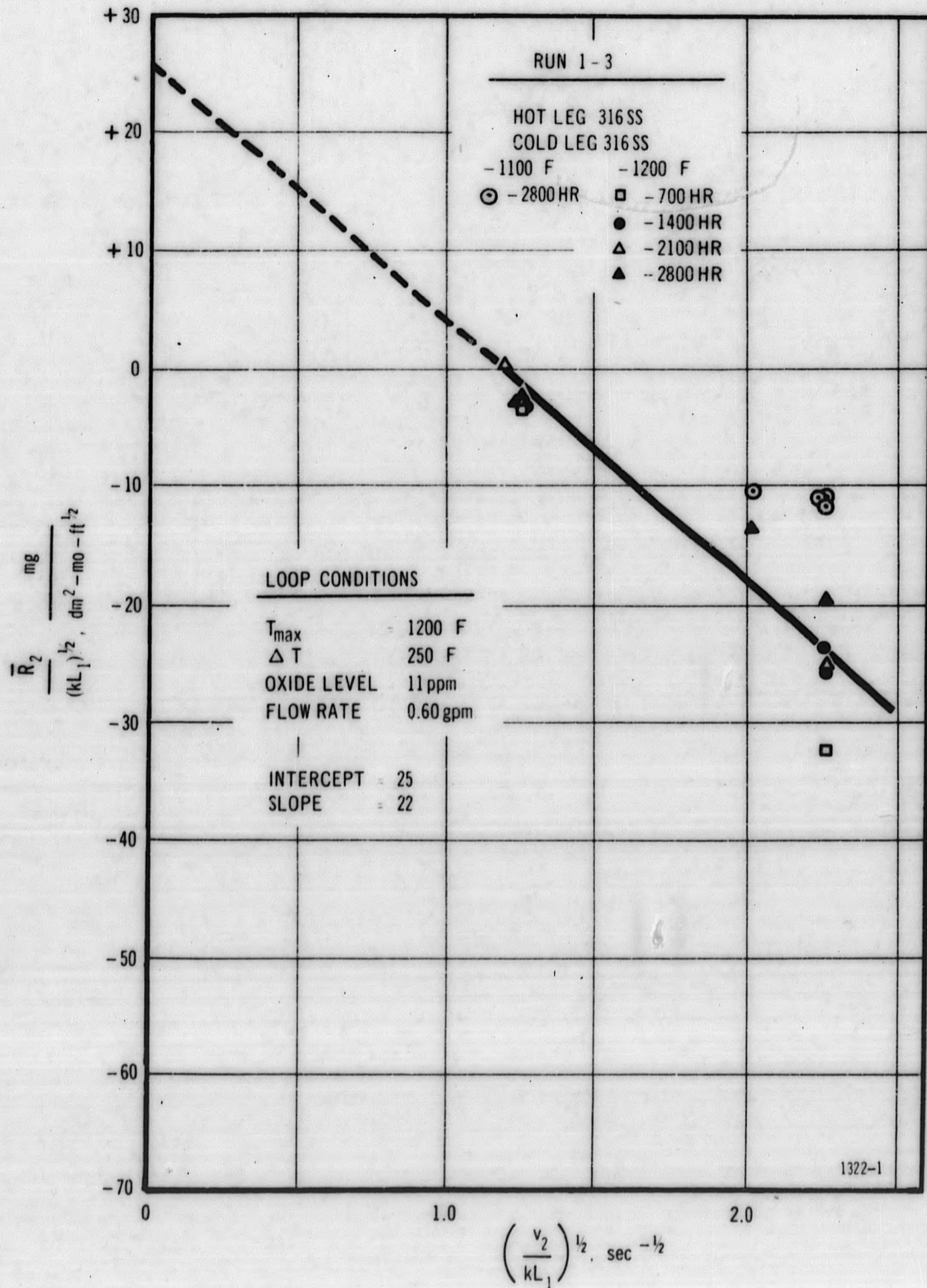


Figure 5. Corrosion Data Correlation - Run 1-3

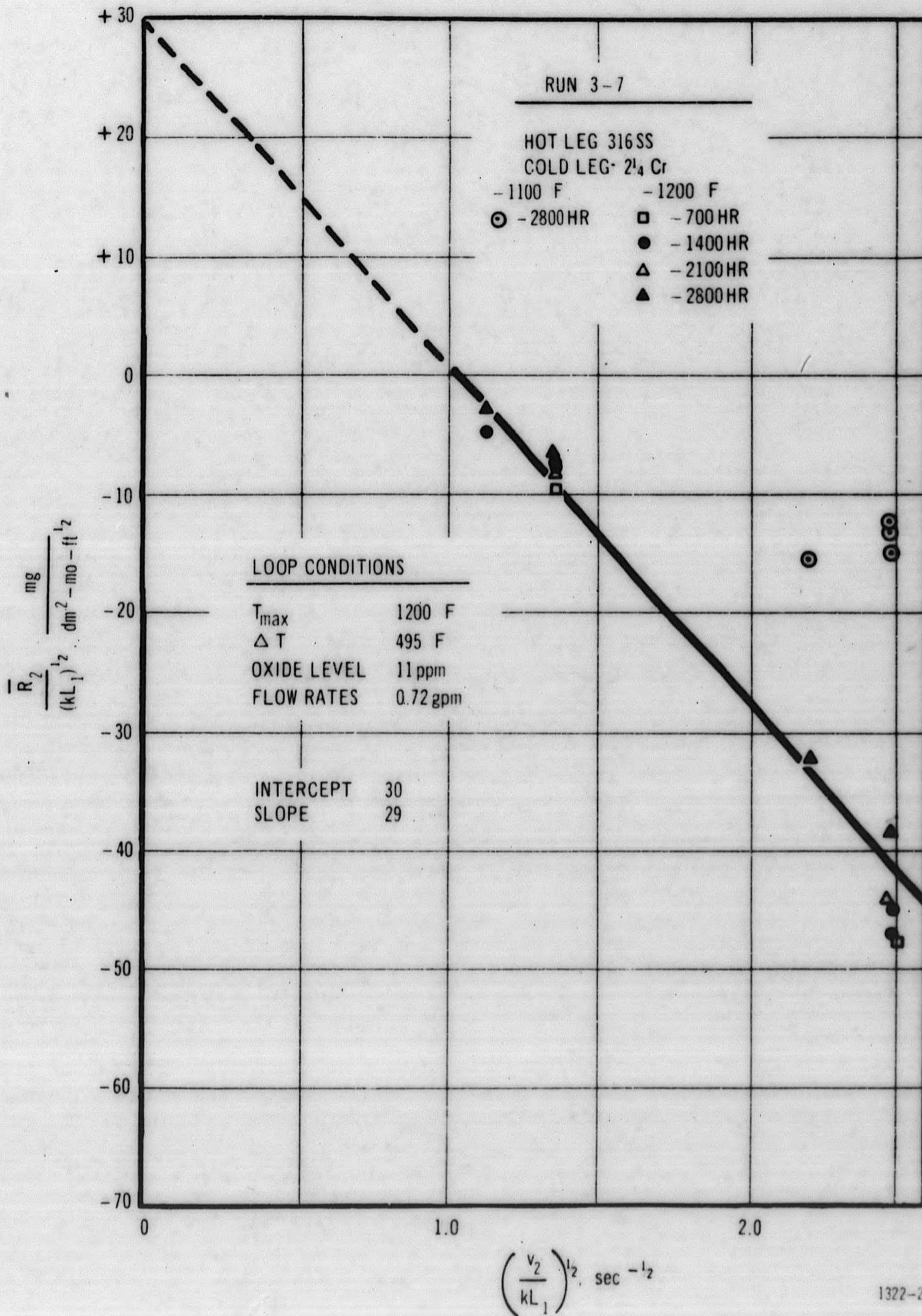


Figure 6. Corrosion Data Correlation - Run 3-7

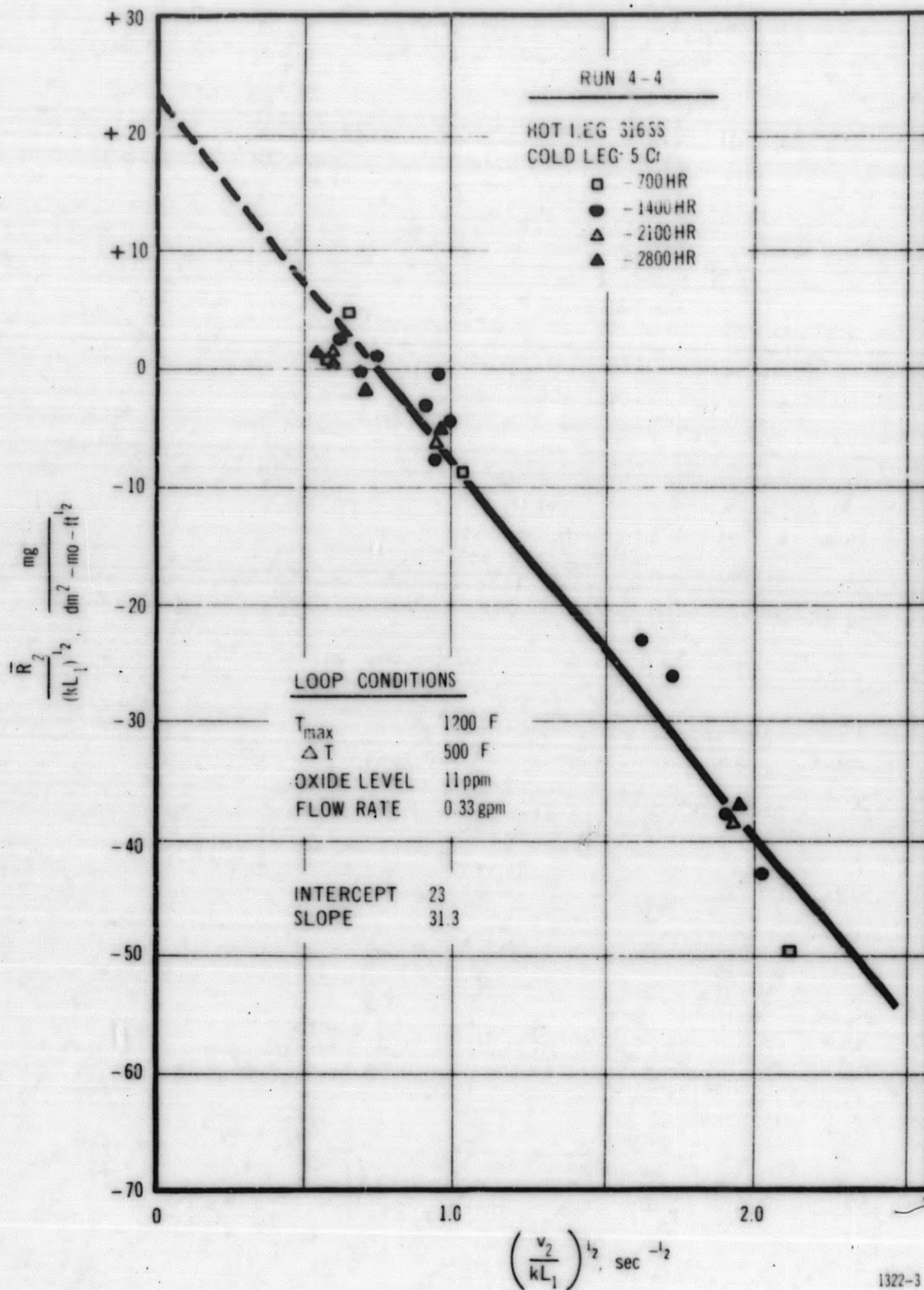


Figure 7. Corrosion Data Correlation - Run 4-4

VI. DISCUSSION OF RESULTS

The fit of the corrosion data to an analytical expression which describes a diffusion mechanism gives sufficient credence to a diffusion process as the rate controlling step and calculations based on this model seem justified. From the slope and intercept of equation (21) the difference between the equilibrium iron oxide concentration at the wall and the entering iron oxide concentration $(C_o - C_{E1}) = \Delta C$ to the isothermal section can be calculated. The purpose of calculating the concentration difference, ΔC , is to show the order of magnitude concentration of the diffusing species in the corrosion process.

The slope of equation (21) equals

$$-2(C_o - C_{E1}) \left(\frac{D}{\pi L_2} \right)^{\frac{1}{2}} \quad (22)$$

The intercept of equation (21) equals

$$8(C_o - C_{E1}) \left(\frac{D}{\pi A_2 L_2} \right)^{\frac{1}{2}} \quad (23)$$

The diffusion coefficient of iron oxide is estimated and the concentration difference, ΔC , is calculated for Runs 1-3, 3-7, and 4-4 (Appendix B). These results are given in Table III.

TABLE III

Run	Calculated ΔC , $\frac{\text{g Fe as FeO}}{\text{g Na}}$		FeO solubility extrapolated NRL data, 1200 F, solution saturated with Na_2O 5.33×10^{-8}
	From Slope	From Intercept	
1-3	0.37×10^{-8}	3.7×10^{-8}	
3-7	0.49×10^{-8}	4.4×10^{-8}	
4-4	0.52×10^{-8}	3.4×10^{-8}	

The ΔC calculated from the intercept is of the same order of magnitude as the extrapolated value of assumed FeO solubility in sodium saturated with sodium oxide. [1] In the particular runs analyzed the amount of sodium oxide in the bulk stream is less than the oxide saturation value and the amount of FeO in solution would be expected to be less than that reported for a solution saturated with sodium oxide. Because the validity of many of the assumptions made in the treatment is uncertain an order of magnitude agreement is all that is desired and this can be observed in Table III.

The understanding of the mechanism of stainless steel or iron corrosion in liquid sodium has suffered in the past because of discrepancies in the reported solubilities of iron in sodium.

The data of Baus, et al., which are used in this paper are a factor of 10^3 less than those of Drugas and Kelman, [3] Mausteller and Batutis, [9] and Epstein, [5]. This discrepancy is unresolved at this time. In fact, iron concentrations in sodium averaged about 3×10^{-6} g Fe/g Na at the sampling temperature of 650 F for Runs 3-7 and 4-4, and 5.0×10^{-6} g Fe/g Na at the sampling temperature of 900 F for Run 1-3. Whether the iron is present as metallic iron, iron oxide, iron carbide, etc., is yet to be determined. The concentration levels of 10^{-8} $\frac{\text{g Fe}}{\text{g Na}}$ of some iron-oxygen compound which is hypothesized seems to agree well with the data of Baus.

The ΔC values calculated from the slopes in Figures 5 through 7 are seen to be a factor of ten less than those calculated from the intercepts. A possible explanation for this arises from the assumptions made concerning the radial velocity distribution in the loop. In the analytical treatment a flat velocity profile equal to the average velocity was assumed throughout the pipe cross section. In the actual system the velocity next to the wall in the region of δ is much less than the average velocity. A corrected velocity, $v_c = 0.01 v_{\text{avg}}$, in equation (21) would then yield a ΔC value approximately equal to that determined from the intercept.

From Figures 5 through 7 the corrosion rate is seen to decrease as the distance downstream becomes greater - the "downstream effect". The corrosion rate approaches zero and in some instances becomes positive. In the model used to describe the corrosion process, positive corrosion rates or weight gains are not accounted for. In the actual system, two hypotheses for weight gains can be postulated. If sodium oxide reacts with iron of the wall to form FeO and the sodium is saturated with FeO, then no mass transfer of wall material can occur since a concentration gradient is not present. The weight gain of the sample specimen is then due to adhering oxide films.

A second mechanism by which a weight gain in downstream positions could occur is as follows: Iron oxide diffuses into the bulk sodium stream where it becomes reduced by sodium to iron. If the solubility of iron in solution is exceeded, then metallic iron deposits out of solution.

An expression for the corrosion rate of a flat plate in which a diffusion process is the controlling step is (see Equation 11) simply $R = A \sqrt{\frac{v}{x}}$ (24)

where R = corrosion rate
 v = average flow velocity
 x = distance downstream
 A = constant

Equation (21) is a modification of this expression and becomes more complicated because system geometry is taken into consideration. The corrosion rate expression for a cylindrical pipe reduces to equation (24) if the residence time of the flowing liquid is short. From equation (24) the effect of the velocity and position on the local corrosion rate can be seen. The corrosion rate at a given position in the loop is proportional to the square root of the flow velocity. At a constant flow velocity the corrosion rate is inversely proportional to the square root of the distance downstream.

The hypothesis that iron oxide is the species which enters directly into the corrosion process is nothing but logical speculation at this time. Experiments to measure and identify the corroding iron species are necessary before the enigma of corrosion mechanism and iron solubility in sodium can be resolved. The lack of fundamental data in this area has reduced the effectiveness of engineering tests performed to date.

VII. CONCLUSIONS

From this study some general conclusions are made on corrosion of iron based systems subjected to flowing sodium.

- a. The controlling mechanism in the corrosion process is hypothesized to be diffusion of some iron-oxygen species.
- b. The corroding species is present in liquid sodium at concentrations of approximately 10^{-8} g Fe/g Na.

VIII. ACKNOWLEDGMENTS

The author thanks Leo F. Epstein for his helpful discussions and comments on corrosion in liquid metal systems and for his review of the material presented in this paper. The author also thanks E. G. Brush for his comments on the manuscript.

APPENDIX A

TABLES OF LOOP OPERATING CONDITIONS AND CORROSION DATA
FOR RUNS 1-3, 3-7, 4-4

TABLE IV

Loop Operating Parameters and Materials of Construction

	<u>Run 1-3</u>	<u>Run 3-7</u>	<u>Run 4-4</u>
Hot Leg Material	316 S.S.	316 S.S.	316 S.S.
Cold Leg Material	316 S.S.	2 $\frac{1}{4}$ Cr - 1 Mo	5 Cr - $\frac{1}{2}$ Mo - $\frac{1}{2}$ Ti
T _{max.} , °F	1200	1200	1200
ΔT, °F	250	500	500
Flow rate, gpm	0.60	0.72	0.33
Oxide Level, ppm	11	11	11

TABLE V

Run 1-3 Sample Location and Corrosion Rates

x = 0 at H3 Heater Inlet

Location	Position		Velocity		Temp °F	Time hr.	R mg dm ² -mo.	k	R √kL ₁	√v ₂ √kL ₁
	L ₁ , ft.	L ₁ ^{1/2}	v ₂ , ft sec	v ₂ ^{1/2}						
H3 in	1.28	1.13	6.6	2.57	1200	700	- 36.3	1	- 32.2	2.28
	1.28	1.13	6.6	2.57	1200	1405	- 29.2	1	- 25.8	2.28
	1.28	1.13	6.6	2.57	1200	1411	- 26.3	1	- 23.2	2.28
	1.28	1.13	6.6	2.57	1200	2116	- 28.8	1	- 25.5	2.28
	1.28	1.13	6.6	2.57	1200	2816	- 22.2	1	- 19.6	2.28
H3 out	1.62	1.27	19.7	4.45	1200	2816	- 29.5	3	- 13.5	2.02
H3R in	4.28	2.06	6.6	2.57	1200	700	- 12.7	1	- 6.19	1.25
	4.28	2.06	6.6	2.57	1200	1405	- 5.4	1	- 2.62	1.25
	4.28	2.06	6.6	2.57	1200	1411	- 7.1	1	- 3.43	1.25
	4.28	2.06	6.6	2.57	1200	2116	- 6.0	1	- 2.88	1.25
	4.28	2.06	6.6	2.57	1200	2816	- 4.6	1	- 2.23	1.25
H3R out	4.63	2.16	19.7	4.45	1200	2816	+ 0.4	3	+ 0.01	1.19
H2 in	1.28	1.13	6.6	2.57	1100	2816	- 12.3	1	- 10.9	2.29
	1.28	1.13	6.6	2.57	1100	2816	- 12.5	1	- 11.0	2.29
	1.28	1.13	6.6	2.57	1100	2816	- 12.6	1	- 11.1	2.29
H2 out	1.62	1.27	19.7	4.45	1100	2816	- 23.4	3	- 10.6	2.02

TABLE VI

Run 3-7 Sample Location and Corrosion Rates

x = 0 at H3 Heater Inlet

Location	Position		Velocity		Time hr.	Temp °F	R mg dm ² -mo.	k	$\frac{R}{\sqrt{kL_1}}$	$\sqrt{\frac{v_2}{kL_1}}$
	L ₁ , ft.	L ₁ ^{1/2}	v ₂ , ft sec	v ₂ ^{1/2}						
H3 in	1.28	1.13	8.0	2.83	710	1200	- 54.1	1	- 48.0	2.50
	1.28	1.13	7.9	2.81	1446	1200	- 53.8	1	- 47.5	2.49
	1.28	1.13	7.9	2.81	1367	1200	- 51.1	1	- 45.4	2.49
	1.28	1.13	7.8	2.80	2103	1200	- 50.1	1	- 44.5	2.48
	1.28	1.13	7.9	2.81	2813	1200	- 43.8	1	- 38.8	2.49
H3 out	1.62	1.27	23.7	4.88	2813	1200	- 71.1	3	- 32.4	2.22
H3R in	4.28	2.06	8.0	2.83	710	1200	- 20.5	1	- 9.93	1.37
	4.28	2.06	7.9	2.81	1446	1200	- 15.6	1	- 7.59	1.36
	4.28	2.06	7.9	2.81	1367	1200	- 15.8	1	- 7.63	1.36
	4.28	2.06	7.8	2.80	2103	1200	- 16.7	1	- 8.10	1.35
	4.28	2.06	7.9	2.81	2813	1200	- 13.5	1	- 6.57	1.36
H3R out	4.63	2.16	11.9	3.45	1367	1200	- 15.0	2	- 4.90	1.13
	4.63	2.16	11.9	3.45	2813	1200	- 9.4	2	- 3.06	1.13
H2 in	1.28	1.13	7.9	2.81	2813	1100	- 15.2	1	- 13.4	2.49
	1.28	1.13	7.9	2.81	2813	1100	- 13.8	1	- 12.2	2.49
	1.28	1.13	7.9	2.81	2813	1100	- 17.2	1	- 15.2	2.49
H2 out	1.62	1.27	23.7	4.88	2813	1100	- 34.8	3	- 15.9	2.22

TABLE VII

Run 4-4 Sample Location and Corrosion Rates

x = 0 at 1100 F Position in H1 Heater

Location	Position		Velocity		Time hrs.	Temp °F	R mg. dm ² -mo.	k	R $\sqrt{kL_1}$	$\sqrt{v_2}$ $\sqrt{kL_1}$
	L ₁ , ft.	L ₁ ^{1/2}	v ₂ , ft/sec	v ₂ ^{1/2}						
H1 in	0.91	0.96	4.13	2.04	700	1200	- 47.9	1	- 49.8	2.13
	0.91	0.96	3.85	1.96	1400	1200	- 41.5	1	- 43.2	2.04
	0.91	0.96	3.4	1.84	1409	1200	- 36.6	1	- 38.1	1.92
	0.91	0.96	3.5	1.87	2109	1200	- 37.1	1	- 38.8	1.95
	0.91	0.96	3.6	1.90	2809	1200	- 35.8	1	- 37.2	1.97
H1 out	1.26	1.13	11.5	3.40	1400	1200	- 52.3	3	- 26.8	1.74
	1.26	1.13	10.3	3.20	1409	1200	- 45.1	3	- 23.2	1.64
H2 in	3.82	1.96	4.13	2.04	700	1200	- 17.4	1	- 8.89	1.04
	3.82	1.96	3.85	1.96	1400	1200	- 9.36	1	- 4.77	1.00
	3.82	1.96	3.4	1.84	1409	1200	- 15.7	1	- 8.00	0.94
	3.82	1.96	3.5	1.87	2109	1200	- 12.9	1	- 6.60	0.95
	3.82	1.96	3.6	1.90	2809	1200	- 10.3	1	- 5.28	0.97
H2 out	4.15	2.04	11.5	3.40	1400	1200	- 2.52	3	- 0.60	0.96
	4.15	2.04	10.3	3.20	1409	1200	- 11.5	3	- 3.26	0.91
H3 out	7.05	2.66	11.5	3.40	1400	1200	+ 4.82	3	+ 1.05	0.74
	7.05	2.66	10.3	3.20	1409	1200	- 1.56	3	- 0.34	0.69
	7.05	2.66	10.9	3.30	2809	1200	- 9.15	3	- 1.99	0.71
H3R in	9.68	3.12	4.13	2.04	700	1200	+ 14.5	1	+ 4.65	0.65
	9.68	3.12	3.85	1.96	1400	1200	+ 7.06	1	+ 2.26	0.63
	9.68	3.12	3.4	1.84	1409	1200	+ 2.68	1	+ 0.86	0.59
	9.68	3.12	3.5	1.87	2109	1200	+ 2.78	1	+ 0.89	0.60
	9.68	3.12	3.6	1.90	2809	1200	+ 3.50	1	+ 1.12	0.61
H3R out	10.05	3.16	10.9	3.30	2809	1200	+ 4.33	3	+ 0.79	0.60

APPENDIX B

CALCULATIONS OF DIFFUSIONCOEFFICIENT AND CONCENTRATIONS OF IRON OXIDE IN SODIUM1. Diffusion Coefficient

The self-diffusion coefficient of sodium is given by the expression^[10]

$$D_{\text{Na}} = 1.10 \times 10^{-3} e^{-\frac{2450}{RT}} \frac{\text{cm}^2}{\text{sec}} \quad \text{where } T \text{ is in } ^\circ\text{K}$$

At 1200 F $D_{\text{Na}} = 2.9 \times 10^{-4} \text{ cm}^2/\text{sec}.$

To a first approximation the diffusion coefficient of iron oxide, D_{FeO} , in liquid sodium can be calculated by the following expression

$$\frac{D_{\text{FeO}}}{D_{\text{Na}}} \cong \sqrt{\frac{M_{\text{Na}}}{M_{\text{FeO}}}}$$

where $M_{\text{Na}} = \text{molecular weight of sodium} = 23$

$M_{\text{FeO}} = \text{molecular weight of iron oxide} = 72$

$$D_{\text{FeO}} = 2.9 \times 10^{-4} \sqrt{\frac{23}{72}} = 1.65 \times 10^{-4} \text{ cm}^2/\text{sec. at } 1200^\circ\text{F.}$$

2. Iron Oxide Concentration

From equation (21) the slope of the plot of $\frac{R}{(kL_1)^{\frac{1}{2}}}$ versus $\left(\frac{v_2}{kL_1}\right)^{\frac{1}{2}}$ equals

$$-2(C_0 - C_{E1}) \left(\frac{D}{\pi L_2}\right)^{\frac{1}{2}}$$

The intercept of the same plot equals

$$8(C_0 - C_{E1}) \frac{D}{(\pi A_2 L_2)^{\frac{1}{2}}}$$

From Figures 5 through 7, values of the slopes and intercepts are determined and the ΔC calculated. These results are given in Table VIII.

TABLE VIII

Calculated Concentration Difference Values (ΔC) = $(C_o - C_{E1})$

Run	Slope	$\frac{\text{g Fe as FeO}}{\text{cm}^3}$	$\frac{\text{g Fe as FeO}}{\text{g Na}}$	Intercept	$\frac{\text{g Fe as FeO}}{\text{cm}^3}$	$\frac{\text{g Fe as FeO}}{\text{g Na}}$
1-3	-22	2.9×10^{-9}	3.7×10^{-9}	25	2.9×10^{-8}	3.7×10^{-8}
3-7	-29	3.9×10^{-9}	4.9×10^{-9}	30	3.5×10^{-8}	4.4×10^{-8}
4-4	-31	4.1×10^{-9}	5.2×10^{-9}	23	2.7×10^{-8}	3.4×10^{-8}

From the value of the slope

$$\Delta C = \frac{\text{slope}}{-2} \frac{(\pi L_2)^{\frac{1}{2}}}{D_{\text{FeO}}^{\frac{1}{2}} \times \text{C. F.}}$$

L_2 = length of sample specimen = 2.94 inches

D_{FeO} = diffusion coefficient of FeO in sodium at 1200 F

$$= 1.65 \times 10^{-4} \text{ cm}^2/\text{sec.}$$

$$\text{C. F.} = \text{conversion factor} = 1.40 \times 10^{+12} \frac{\text{mg}}{\text{dm}^2 \text{-mo-ft}^{\frac{1}{2}}} / \frac{\text{g}}{\text{cm}^2 \text{-sec-cm}^{\frac{1}{2}}}$$

From the value of the intercept

$$\Delta C = \frac{\text{intercept}}{8} \frac{(\pi A_2 L_2)^{\frac{1}{2}}}{D \times \text{C. F.}}$$

Where A_2 = total flow cross section area in sample holder for inlet slots

$$= 0.0309 \text{ square inch}$$

$$\therefore \Delta C = \frac{\text{slope}}{2} \frac{(3.14 \times 2.94 \times 2.54)^{\frac{1}{2}}}{1.29 \times 10^{-2} \times 1.4 \times 10^{+12}}$$

$$= \text{slope } 1.33 \times 10^{-10} \frac{\text{g Fe as FeO}}{\text{cm}^3}$$

$$\text{Also } \Delta C = \frac{\text{intercept } (3.14 \times 0.0309 \times 2.94 \times 16.4)^{\frac{1}{2}}}{8 \times 1.65 \times 10^{-4} \times 1.4 \times 10^{+12}}$$

$$= \text{intercept } 1.17 \times 10^{-9}, \frac{\text{g Fe as FeO}}{\text{cc}}$$

ΔC values as $\frac{\text{g Fe as FeO}}{\text{g Na}}$ are calculated from the density of Na at 1200 F = 0.79 g/cc. [1]

NOMENCLATURE

A_1	=	flow cross-sectional area of section I (length) ²
A_2	=	flow cross-sectional area of section II or sample holder (length) ²
b	=	ratio of cross-sectional areas of section I to section II = A_1/A_2
C	=	concentration of iron oxide as a function of x , g/cm ³
C_{E1}	=	concentration of iron oxide in sodium entering section I at $x = 0$, g/cm ³
C_{E2}	=	concentration of iron oxide in sodium entering section II, g/cm ³
C_o	=	equilibrium iron oxide concentration at the wall of the pipe or sample specimen, g/cm ³
ΔC	=	concentration difference ($C_o - C_{E1}$) g/cm ³
d_1	=	effective cross section diameter of section I.
D, D_{FeO}	=	diffusion coefficient of iron oxide in sodium, cm ² /sec.
D_{Na}	=	self diffusion coefficient of sodium, cm ² /sec.
k	=	geometry factor for a particular sample position (see equation [19]) dimensionless.
L_1	=	length of section I. (length)
L_2	=	length of sample specimen. (length)
M	=	molecular weight
N_x	=	mass flux of iron oxide in x direction, g/cm ² -sec.
N_y	=	mass flux of iron oxide in y direction, g/cm ² -sec.
N_{Na_x}	=	mass flux of sodium in x direction, g/cm ² -sec.
$R(x)_1$	=	local corrosion rate in section I as a function of distance in x -direction, g/cm ² -sec.
$R(x)_2$	=	local corrosion rate of sample specimen as a function of distance in x -direction, g/cm ² -sec.
\bar{R}_1	=	average corrosion rate in section I, g/cm ² -sec. or mg/dm ² -mo.
\bar{R}_2	=	average corrosion rate in section II, g/cm ² -sec. or mg/dm ² -mo.
S	=	surface area exposed to corrosion, section I (length)
t	=	thickness of sample specimen or pipe wall. (length)
v_1	=	average flow velocity in section I (length/time)
v_2	=	average flow velocity in section II (length/time)
w	=	width of differential volume element, cm
x	=	distance in direction of sodium flow, (length)
y	=	distance perpendicular to direction of sodium flow (length)
z	=	mass fraction of iron oxide
$\text{erf } x$	=	$(2/\sqrt{\pi}) \int_0^x e^{-p^2} dp$

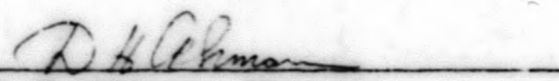
REFERENCES

1. Baus, R. A., et al.: "The Solubility of Structural Materials in Sodium." Proceedings of the International Conference on the Peaceful Uses of Atomic Energy. Held in Geneva, August, 1955, Vol. 9, United Nations Publications, New York, 1956.
2. Bird, R. B., Stewart, W. E., and Lightfoot, E. N., "Transport Phenomena", John Wiley and Sons, Incorporated. New York, 1960.
3. Drugas, P. G., and Kelman, L. R., "Equipment and Procedures for Studying the Equilibrium Solubility of Iron in NaK". ANL-5359, September 1953.
4. Epstein, L. F., "Static and Dynamic Corrosion and Mass Transfer in Liquid Metal Systems", Chemical Engineering Progress Symposium Series, No. 20, Vol. 53, 1957.
5. Epstein, L. F., "Preliminary Studies on the Solubility of Iron in Liquid Sodium", Science 112, 426, 1950.
6. Horsley, G. W., A. E. R. E. M/R-1441. Department of Atomic Energy, Harwell, Berks, Great Britain, April 1954; J. Iron Steel Inst. (London), 182, 43, January 1956.
7. Lockhart, R. W., Billuris, G., and Lane, M. R., "Sodium Mass Transfer: I - Test Loop Design", GEAP-3725, AEC Research and Development Report, June 1962.
8. Pohl, L. E., "Sodium Mass Transfer: IV, 1962 Corrosion Sample Data", GEAP-4181, January 1963.
9. Mausteller, J. W., and Batutis, E. F., "Mine Safety Appliance Company," Technical Report 36, March 1955.
10. Meyer, R. E., and Nachtrieb, N. H., J. Chem. Phys., 23, 405, 1955.
11. "Liquid Metals Handbook, Sodium-NaK Supplement", 3rd Edition, July 1955.

GEAP-4313

APPROVED BY:


R. W. Lockhart, Project Engineer
Sodium Mass Transfer Project


D. H. Ahmann, Manager
Chemistry and Chemical Engineering

ATOMIC POWER EQUIPMENT DEPARTMENT
GENERAL ELECTRIC
SAN JOSE, CALIFORNIA

END